Pergamon

Tetrahedron 58 (2002) 7975–7982

TETRAHEDRON

New ligand combinations for the efficient stabilization of short nucleic acid hairpins

Justine Michel,[a] Katell Bathany,[b] Jean-Marie Schmitter,[b] Jean-Pierre Monti[c] and Serge Moreau[a,*]

[a]*IFR Pathologies Infectieuses, INSERM U-386, Bat 3a, Université Victor Segalen Bordeaux 2,146 rue Léo Saignat, 33076 Bordeaux, France*
[b]*Institut Européen de Chimie et Biologie, FRE CNRS 2247, 16, avenue Pey Berland, 33607 Pessac, France*
[c]*UFR Sciences Pharmaceutiques EA 491, Université Victor Segalen, 146 rue Léo Saignat, 33076 Bordeaux, France*

Received 15 April 2002; revised 14 June 2002; accepted 15 July 2002

Abstract—Short nucleic acid hairpins (one or two base-pair stems) were strongly stabilized by simple chemical modifications. Non-nucleosidic pyrene or naphtalene diimide derivatives were appended at both 3′ and 5′ nearby ends of 2′-OMe RNA hairpins, yielding a very large increase in melting temperatures of the modified structures (from +21 to +55°C). The excimer formation between the two consecutive pyrene units is in favor of end-stacked pyrenyl rings. © 2002 Published by Elsevier Science Ltd.

1. Introduction

The factors contributing to the thermodynamic stability of DNA or RNA double helices include hydrogen bonding and base stacking. Both are important in stabilizing non-covalent interactions of nucleic acid complexes. An initial experimental estimation which relies on terminal unpaired bases was made on RNA strands and concluded in a relatively equal contribution of base stacking and hydrogen bonding to the stability of a base pair.[1] Intercalation of heteroaromatic rings between two base pairs in a DNA double helix is a well-known example of the stacking properties of flat aromatic structures.[2] Our aim was to develop the combination of flat aromatic rings enabling the stabilization of very short double strands (one or two base pairs) through end-stacking. By looking for synthetic derivatives which might exhibit such properties, we investigated a pyrene system which is thought to improve duplex stability when appended to 3′ or 5′ oligonucleotides ends.[3] We also examined the properties of a naphtalene-tetracarboxylic diimide derived compound which has been shown to allow the construction of stacked aromatic cores.[4] Furthermore, examination of the fluorescence properties of pyrene should allow their stacking arrangement to be checked.[5] The conjugation of these aromatic cycles to short nucleic acid oligomers was performed by using an appropriately functionalized serinol backbone as a minimal nucleotide replacement unit.[6] The phosphoramidite of derivatives **P** and **N** featuring either a pyrene or a naphtalene were synthesized and used in the chemical synthesis of nucleic acid sequences.

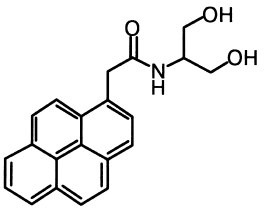

P

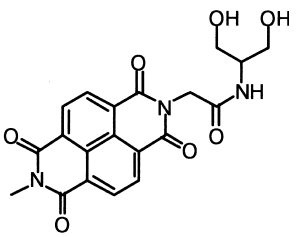

N

Herein we examined the stacking properties of various end combinations of these two aromatic cycles on short-stem loop oligomers, which are potential ligands of TAR (an RNA structural element of the HIV genome).[7]

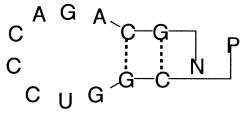

We expected these ligands to be stabilized through the formation of a closed hairpin, as shown on the hypothetical diagram shown above.

2. Chemical synthesis

The synthetic routes for the diols **P** and **N** and their corresponding phosphoramidites are depicted in Scheme 1. The non-symmetrical diimide compound **1** was obtained by successive addition of 0.5 equiv. of glycine aminoacid and a slight excess of methylamine to a solution of the commercially available naphtalenedianhydride in DMF. The crude acid **1** was isolated by acidic precipitation and

Keywords: nucleic acid hairpins; stacking interactions; naphtalene diimide; pyrene derivatives; fluorescence; excimer.

* Corresponding author. Tel.: +33-5-57-5710-16; fax: +33-5-57-5710-15; e-mail: serge.moreau@bordeaux.inserm.fr

0040–4020/02/$ - see front matter © 2002 Published by Elsevier Science Ltd.
PII: S0040-4020(02)00876-1

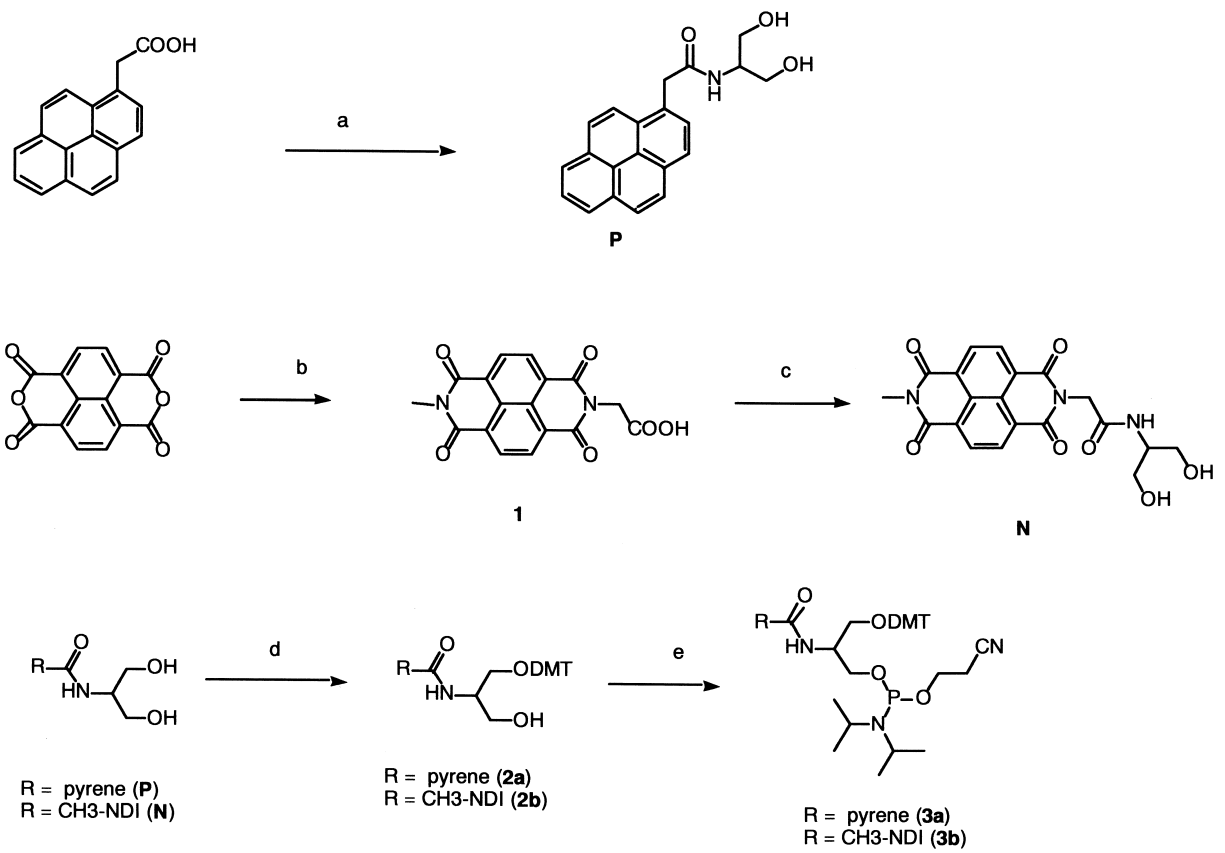

Scheme 1. Chemical synthetic pathway for N and P compounds and their corresponding phosphoramidites. (a) HOBt, DIPC, DMF, rt, 10 min, then Serinol, DIEA, 40°C, 16 h. (b) Glycine, DIEA, DMF, 90°C, 16 h then CH_3NH_2, rt, 3 h. (c) PyBOP, HOBt, TEA, Serinol, DMF 40°C, 3 h. (d) DMTCl, pyridine, rt, 2 h. (e) 2-Cyano-*N*,*N*-diisopropylphosphoramidochloridite, DIEA, CH2Cl2, rt, 1 h.

then used without further purification. The coupling of either 2-pyrene acetic acid or **1** to serinol easily yielded the **P** and **N** diols which were purified through flash chromatography. The corresponding phosphoramidites **3a** and **3b** were obtained by using classical procedures in two steps. First a monotritylation using 1 equiv. of 4,4′-dimethoxytrityl chloride followed by flash silicagel chromatography yielded the monotritylated compounds **2a** and **2b**. Second a phosphitylation reaction with 2-cyanoethyl-*N*,*N*-diisopropylchloro-phosphoramidite in the presence of *N*,*N*-diisopropylethylamine afforded the desired compounds **3a** and **3b**. These compounds are obtained as mixtures of stereoisomers and are used as such in solid phase nucleic acid synthesis. The structures of these various compounds were checked by mass spectrometry (FAB) and NMR spectrometry (^{1}H, ^{13}C and ^{31}P). All the spectral characteristics of these compounds are given in Section 8.

3. Oligonucleotide synthesis

The phosphoramidites of **N** and **P** were used to incorporate the two aromatic nuclei into oligonucleotide sequences. The oligomer sequences were conceived from previous data on the characterization of aptameric ligands for the TAR RNA[7] and were constructed using 2′-O-Me RNA nucleoside units. The synthesized oligomeric sequences are shown in Table 1. The standard solid phase synthesis procedure was used to couple the various phosphoramidite monomers. The coupling times of the monomer **P** and **N** were increased to 15 min. Under these conditions the coupling yields were similar to those of standard 2′-O-Me monomers, as estimated from the detritylation profiles. For the 3′ conjugation of **N** and **P** monomers, a universal support (commercially available from Glen Research) was used. In order to eliminate any amine reactions on the diimide groups of **N**,[8] a sodium hydroxide deprotection procedure was chosen, avoiding prolonged contact with the amine groups. In all cases the chemical integrity of the oligomers was checked by MALDI-TOF mass spectra analysis (Table 1).

4. Hairpin stability

The contributions of **N** and **P** moieties to the stability of the hairpins were analyzed by using UV thermal denaturation experiments. The oligomers H10 and H12 may fold as hairpins with short stems of 1–2 base pairs. As expected these oligonucleotides exhibited a single transition in UV thermal monitored melting experiments. Experiments conducted on H12 and 12P5P3 oligomers at concentrations ranging from 0.5 to 7.5 μM revealed no variations in T_m data (50±1°C for H12 and 72±1°C for 12P5P3. This is indicative of a monomolecular equilibrium, thus showing that the observed T_m are related to the fusion of a hairpin

Table 1. Hairpin sequences

Id[a]	Oligonucleotide sequences[b]	Calcd mass	Found	T_m (ΔT_m) 260 nm[c]	H% (T_m) 343 nm[d]
H12	CGGUCCCAGACG	nd	nd	50.0	
H10	GGUCCCAGAC	nd	nd	20.0	
12P3	CGGUCCCAGACG**P**	4370.8	4372.2	66.5 (16.5)	13
12N3	CGGUCCCAGACG**N**	4450.0	4442.3	62.0 (12.0)	
12P5	**P**CGGUCCCAGACG	4342.0	4344.7	60.0 (10.0)	10 (60.0)
12N5	**N**CGGUCCCAGACG	4418.8	4419.9	50.0 (0.0)	
12P5P3	**P**CGGUCCCAGACG**P**	4767.4	4771.4	72.0 (21.0)	19 (72.0)
12N5N3	**N**CGGUCCCAGACG**N**	4928.3	4929.4	>70.0 (>21.0)	
12N5P3	**N**CGGUCCCAGACG**P**	4845.4	4848.5	70.0 (21.0)	
12P5N3	**P**CGGUCCCAGACG**N**	4845.4	4850.7	62.0 (12.0)	
10P5	**P**GGUCCCAGAC	3663.6	3665.1	41.5 (21.5)	nd
10P3	GGUCCCAGAC**P**	4088.9	4089.8	62.0 (42.0)	16 (62.0)
10P5P3	**P**GGUCCCAGAC**P**	4767.4	4771.4	66.0 (46.0)	16 (67)
10PP5P3	**PP**GGUCCCAGAC**P**	4484.3	4490.7	75.0 (55.0)	13
10P5PP3	**P**GGUCCCAGAC**PP**	4484.3	4484.3	75.0 (55.0)	16
H14	5′ACGGUCCCAGACGU3′	4622.9	4631.8	56.0	

[a] Id: identification of oligonucleotides. The number stands for the length of the oligomer; the letters P and N stand for the ligands pyrene and NDI, respectively. 5 and 3 indicate the substituted end(s).
[b] Complementary base pairs are underlined.
[c] The melting temperature T_m (±0.5°C) was obtained under the conditions described in Section 8. $\Delta T_m = T_m$(modified oligomers) − T_m(unmodified parent hairpin). The unmodified hairpins used as references are termed H10 for 10-mer sequences and H12 for 12-mer sequences.
[d] H%: percent of hyperchromism observed at 343 nm (nd: not determined).

structure and not a bulged duplex. In the following experiments, T_m data were recorded at a 1 μM concentration of oligomers. The H10 hairpin, although showing a weakly cooperative curve, was characterized by a melting transition at 20°C. All the 3′ or 5′ modified hairpins except oligomer 12N5 exhibited a very significant increase in T_m relative to the corresponding unmodified ones. Thus, a single pyrene residue in the 3′ position of H10 or H12 resulted in a ΔT_m of +42 and +16.5°C, respectively (10P3, 12P3, Table 1). Multiple **N** or **P** substitutions at 3′ and 5′ revealed even higher increases since ΔT_m values of +55.0°C could be reached with the combination of three **P** at 3′ and 5′ ends of H10 (see 10PP5P3, 10P5PP3, Table 1). When monitored at 343 nm, the long wavelength absorption band of the pyrene cycle, the UV thermal denaturation experiments on 12P5 and 12P5P3 revealed a significant hyperchromic contribution (10 and 19%, respectively). In the latter cases, T_ms were observed at the same values as those at 260 nm (Table 1). The hyperchromic effect was always significant at 343 nm, but a clear cooperative transition was not always detected for some oligomers, thereby preventing a clear-cut melting transition to be determined at this wavelength (Table 1).

5. Fluorescence studies

The fluorescence properties of pyrene were used to check for the stacked arrangements of the chromophores. Upon excitation at 349 nm, the 12P3 oligomer showed a fluorescence emission characteristic of a monomer (two main peaks at 379 and 395 nm and a weak shoulder at 421 nm[5] (Fig. 1(a)). Similar results were observed for 12P5. The 12P5P3 hairpin, which incorporates two nearby pyrenes, exhibited fluorescence emission properties indicative of excimer formation. When excited at 349 nm, the hairpin emission spectra showed a new broad band centered at 485 nm, together with the monomer emission bands (Fig. 1(b)). The ratio of intensities (I_E/I_M) of excimer emission (485 nm) to that of the monomer (379 nm) was 0.88. The 10P5P3 hairpin exhibited similar fluorescence features with a ratio I_E/I_M rising to 5.7. The tris pyrenyl conjugates 10PP5P3, 10P5PP3 spectra were almost entirely constituted by excimer emission (Fig. 1(c)).

6. Molecular modeling studies

To further understand the structures of our hairpin species, we conducted molecular mechanics studies. Our objective was to evaluate the stacking or intercalating abilities of the **P** and **N** pending aromatic cycles. To construct a three base-pair model, we chose an RNA double strand mimicking the stem of the H12 hairpin with a terminal CG base pair. **P** and **N** substituents were introduced at the 3′ or 5′ ends. Stacked or intercalated species were constructed. During the minimizations, the base pairs were fully maintained as well as the puckering of the ribose units. The mono-substituted species 3′**P**, 5′**P**, 3′**N**, 5′**N** all proved capable of stacking (Fig. 2(b)) over the last CG pair or of intercalating (Fig. 2(a)) between the first two pairs. The N–CH3 substituent of the NDI nucleus did not prevent intercalation (Fig. 2(a)). According to the fluorescence data, we focused our attention on the bis substituted **P** species, looking at both possible conformations (3′ over 5′, or vice-versa). No particular steric constraints were detected by the minimization calculation, thus indicating very similar energies for both stacked structures. An illustration of possible stacking geometries is shown in Fig. 2(c). The two consecutive **P** units overlap each other, with the stacking area corresponding roughly to 75% of the aromatic pyrene surface.

7. Discussion

The present molecular modeling data indicate that the short flexible linker allows end stacking or intercalation whatever the position or the residue. The experimental data (T_m, hyperchromism) regarding the monosubstituted species are consistent with both intercalation and dangling positions of

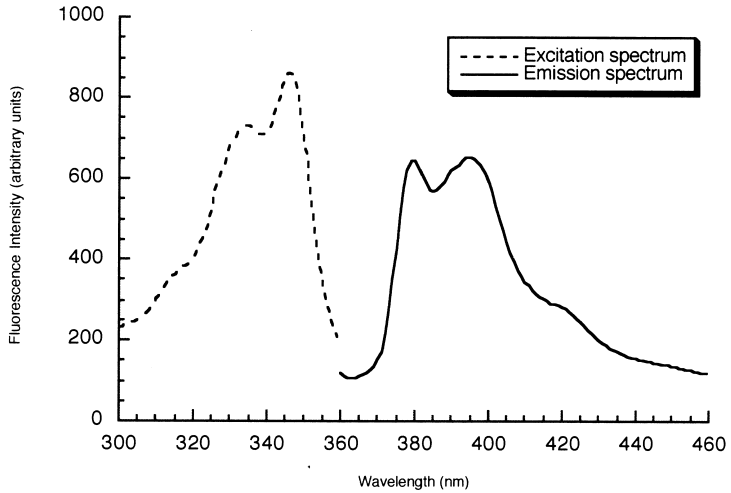

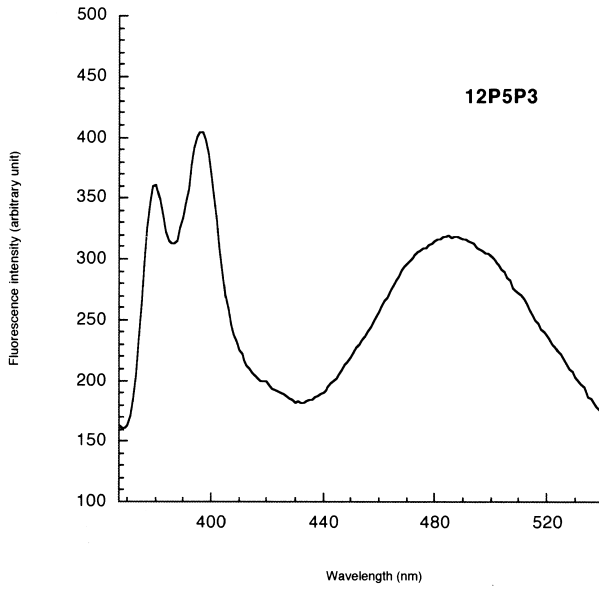

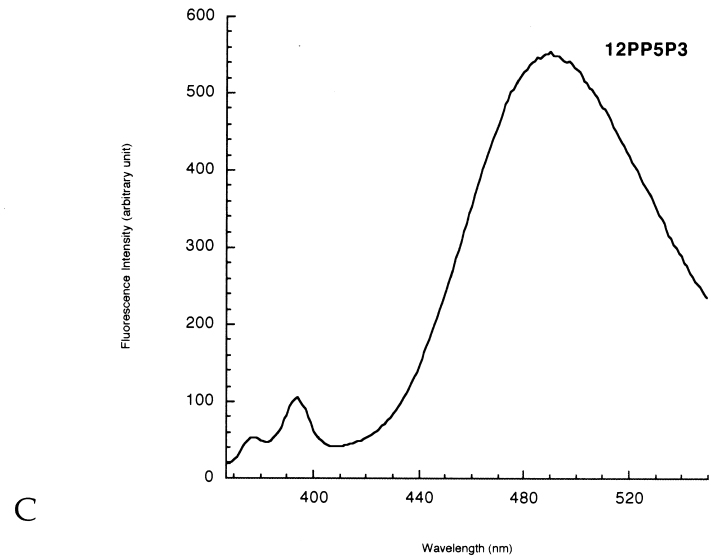

Figure 1. (a) Excitation fluorescence spectrum (- - -) and emission spectrum (__) of hairpin 12P3. The fluorescence excitation was recorded for an emission wavelength set at 379 nm for 0.1 μM of 12P3 in the following buffer: 20 nM sodium cacodylate, 140 mM potassium chloride, 20 mM sodium chloride (pH 7.3), 3 mM magnesium chloride. The emission spectrum (λ_{exc} 349 nm) was obtained under the same conditions. (b) Emission spectrum of 12P5P3 (0.1 μM) (λ_{exc} 349 nm). The IE/IM (0.88) ratio was measured at 379 and 485 nm. (c) Emission spectrum of 10PP5P3 (0.1 μM) (λ_{exc} 349 nm). In both cases the buffer was: 20 nM sodium cacodylate (pH 7.3), 140 mM potassium chloride, 20 mM sodium chloride, 3 mM magnesium chloride.

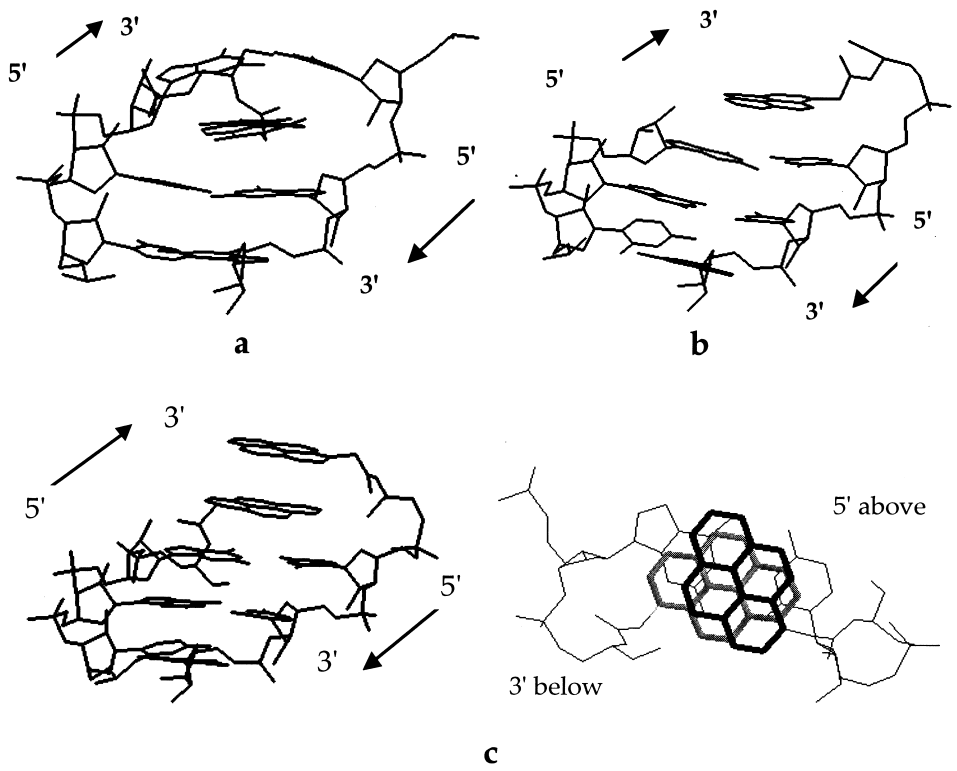

Figure 2. Illustrations of possible intercalating or stacking geometries of **N** or **P** units on the 3 base-pair model used in this study (wireframe representation). (a) Intercalated 3′ NDI unit (view from the major groove). (b) 5′ end stacked pyrene cycle above the last GC pair. (c) Wireframe view of the 3 base-pair model duplex with the 2 stacked pyrenyl units. Left: view from the major groove. Right: view looking down the helical axis, dark bold is the 5′ P unit, light bold is the 3′ P unit above the last GC pair (wireframe).

P and **N** residues. Therefore, it is not possible to decide which of the two hypotheses is more likely and cannot rule out the occurrence of an equilibrium between the two structures. NMR structural studies would have to be conducted to obtain further experimental evidence.

3′ or 5′ substitutions revealed different contributions. Whatever the residue, the 3′ position provided more efficient stabilization with the non-polar pyrene residue being the best one in this case. Such observations have been reported for various non-natural nucleosides at the 5′ end of DNA duplexes. For example it has been shown that the best stacking is obtained with non-polar molecules through the hydrophobic effect.[3] Newcomb and Gellman demonstrated that optimal stacking properties can be reached between polar and apolar aromatic rings.[9] Geometrical analysis of our structure failed to indicate significant differences in the overlap surfaces of 3′ or 5′ positions (not shown).

Simultaneous substitutions at 5′ and 3′ generally led to an additional stabilization of the hairpins, revealing interactions between the substituents. Thus the two opposing pyrene units might constitute an attractive interstrand contribution, as can be inferred from the fluorescence data. The formation of an excimer revealed the occurrence of stacked interactions between the pyrenyl nuclei. The ratio of intensities of excimer emission to monomer emission was significantly different for H12 or H10 derivatives (a relative increase of 5.7-fold was observed in the latter case). This suggests first a ground state dimer association of the pyrenes and therefore a better arrangement of the stacked pyrenes for the H10 derivatized hairpin.[5] The fluorescence data of the tris pyrenyl derivatives (10PP5P3, 10P5PP3) reinforce these conclusions since almost only excimer emissions were observed in these hairpins. Taken together, these data (T_m, hyperchromism at 343 nm, fluorescence) clearly suggest a successive stacking arrangement of the aromatic cycles above the last base pair of the hairpin stem. Among the four stacked combinations studied here P5P3, N5N3, and N5P3 behave similarly. Additional stabilizations was clearly provided in the case of the bis **N**-substituted hairpin 12N5N3 (ΔT_m=+21°C) in comparison with 12N3 and 12N5 (ΔT_m=+12 and 0°C respectively). A similar situation occurred with 12P5P3 (ΔT_m=+21°C) and 12N5P3 (ΔT_m=+20°C), whereas 12P5N3 did not manifest any additional contribution. Molecular modeling studies on stacked bis pyrenyl entities (Fig. 2) revealed a possible overlap of the pyrenyl cycles. The observed geometry does not fully correspond to the optimum overlap (almost complete) expected for the ground state excimer structure.[5] However, the variations in intensities of excimer emission might be due to variations in the overlap of the aromatic pyrenic rings in the H10 or H12 hairpins and to the relative orientations of the rings. The tris pyrenyl species (10PP5P3, 10PP3P5) led to high excimer emission as the two last pyrenyl units are free to adopt a fully overlapped structure (not shown).

In conclusion, the various substituents introduced at the 3′ or 5′ ends of the hairpin H10 and H12 stabilize the structures. The contribution made by the terminal residues in most cases exceeds that of the additional AU base pair included in the H14 hairpin (a three base-pair stem, last line Table 1).

Thus a T_m of 56°C was observed for this hairpin resulting in an increase of +6°C compared to the H12 hairpin. Appended pyrene residues at the 3′ and 5′ ends of the H10 hairpin (one GC base-pair stem) resulted in a T_m of 66°C (ΔT_m=+46°C in comparison with H10 and +10°C in comparison with H12). A combination of three pyrene units led to an even more stable hairpin (T_m=75°C), 19°C more than the 3 base-pair H14 hairpin. On the whole the polar naphtalene diimide moiety led to a similar stabilization to that provided by the apolar pyrene when conjugated at the two nearby hairpin ends. The major determining factor in such stacked compounds is very probably related to the overlap surface on stacking.[3] Although more polar and more hydrated the naphtalene diimide behaves like a hydrophobic compound. This might be due to its structural analogy with the polar nucleic acid bases, where the polar functional groups lie on the edges rather than on the aromatic faces of the rings.[3]

Although the structural parameters of the various hairpins are not completely defined, the ligands **N** and **P** we used in this study (while leading to stereoisomeric mixtures) make a very high stacking contribution to the stability of double-stranded nucleic acid structures. The interstrand interaction provided by two opposite stacked aromatic ligands can exceed the contribution of two additional base pairs in the duplex stabilization. As mentioned in the introduction, the hairpins used in this study are potential ligands for the TAR RNA structure. Work is in progress to evaluate the biological properties of these modified hairpins. The combination of **N** and **P** derivatives might be a useful tool for the efficient closure of synthetic short-stem oligonucleotides and might potentially impair exonuclease activities. They should be evaluated as substitutes for cyclization in decoy strategies.

8. Experimental

8.1. General

Thin layer chromatography (TLC) was performed on Merck silica gel 60 F254 aluminium-backed plates, and visualization was by UV illumination. Flash chromatography refers to column chromatography performed on a BIOTAGE system. UV spectra were obtained on a KONTRON Uvikon 933 spectrophotometer and IR spectra were measured on a BRUKER FT/IR spectrophotometer. NMR spectra were recorded on a BRUKER AC200 spectrometer working at 200 MHz for ^{1}H, 50.32 MHz for ^{13}C and 81.02 MHz for ^{31}P. The chemical shifts are expressed in ppm using TMS as internal standard (for ^{1}H and ^{13}C data) and 85% H_3PO_4 as external standard (^{31}P data). FABMS spectra and high-resolution FABMS analysis were performed in *m*-nitrobenzyl alcohol on a VG Autospec spectrometer. The mass spectra of modified oligonucleotides were obtained on a MALDI-ToF mass spectrometer (Reflex III, Bruker) operating in the linear mode for negative ion detection and using a mixture of oligonucleotides $d(T_{12})-d(T_{18})$ (Sigma) for external calibration mass spectrometry (Brucker Reflex III). The matrix used was THAP (2,4,6-trihydroxyacetophenone).

8.2. Chemical procedure

8.2.1. *N*-(2-Hydroxy-1-hydroxymethyl)-ethyl-1-yl-acetamide (P). 2-Pyreneacetic acid (500 mg) was dissolved in dimethylformamide (15 ml) and preactivated for 15 minutes at room temperature (rt) with hydroxybenzotriazole (282 mg) and 1.1 equiv. of diisopropylcarbodiimide (327 μl). Then, serinol (173 mg) and 1 equiv. of diisopropylethylamine (327 μl) were added. The reaction was stirred overnight at 40°C. The mixture was concentrated, dissolved in CH_3OH/CH_2Cl_2 (1/2), and washed twice with water. The organic phase was then dried over $MgSO_4$and evaporated. The diol was purified by flash chromatography with a gradient of methanol in dichloromethane to afford **P** (320 mg, yield=50%).

UV (MeOH) λ_{max} (nm) (ε) 339 (76,500), 322 (50,200), 272 (79,700); IR (KBr) 1630 cm^{-1} ^{1}H NMR (200 MHz, DMSO-d_6) δ (ppm): 3.45 (s, 4H, CH_2OH), 3.77 (m, 1H, CH), 4.2 (s, 2H, CH_2CO), 8.1 (m, CH ar). ^{13}C NMR (50.32 MHz, DMSO-d_6) δ (ppm): 40.0 (CH_2CO), 52.9 (CH), 60.0 (CH_2OH), 123.9, 124.1, 124.8, 125.0, 126.1, 126.7, 127.0, 127.3, 127.7 (CHar), 128.6, 128.9, 129.6, 130.3, 120.8, 131.2 (Cquat ar), 170.0 (CO). MS (FAB) *m/z* 334.13 (MH^+); HRMS (FAB) calcd for $C_{21}H_{20}NO_3$ (MH^+) 334.1443, found 334.1437.

8.2.2. *N*-(2-Hydroxy-1-(-*O*-4,4′-dimethoxytritylmethyl-ethyl))-2-pyren-1-yl-acetamide (2a). P (297 mg) was carefully dried by three co-evaporations with pyridine and then dissolved in anhydrous pyridine (15 ml). Dimethoxytritylchloride (1.1 equiv., 334 mg) was added under argon atmosphere and mixed at room temperature for 2 h. The mixture was poured on water and the organic phase was extracted twice with dichloromethane, dried over $MgSO_4$ and concentrated. **2a** was purified by flash chromatography with methanol/dichloromethane/triethylamine, 5/94/1 (v/v/v) to afford pure oil (236 mg, yield=35%).

^{1}H NMR (200 MHz, $CDCl_3$) δ (ppm): 3.0 (d, 2H, CH_2O, d, 1H, OH), 3.14 (dd, 2H, CH_2OH), 3.77 (m, 1H, CH), 3.8 (s, 6H, $2OCH_3$), 4.48 (s, 2H, CH_2CO), 8.23 (m, 9H, CHar); ^{13}C NMR (50.32 MHz, $CDCl_3$) δ (ppm): 41.7 (CH_2CO), 51.7 (CH), 54.8 ($2OCH_3$), 63.3 (CH_2O), 85.7 (Cquat DMT), 112.7, 126.4, 127.5, 126.4, 127 (CHar DMT), 122.7, 123.6, 125.0, 125.2, 126.0, 127.3 (Cquat ar DMT), 122.7, 123.6, 125.0, 125.2, 126.0, 127.3 (CHar pyrene), 128.0, 129.2, 130.5, 130.7, 131.1 (Cquat ar pyrene), 171.5 (CONH). MS (FAB) *m/z* 658.26 (M+Na^+); HRMS (FAB) calcd for $C_{42}H_{37}NNaO_5$ (M+Na^+) 658.2574, found 658.2569.

8.2.3. *N*-(2-Cyanoethoxy(diisopropylamino)-1-(-*O*-4,4′-dimethoxytritylmethyl-ethyl))-2-pyren-1-yl-acetamide (3a). 2a (140 mg) was carefully dried by three co-evaporations with pyridine and then was diluted in anhydrous dichloromethane (2 ml, stabilised with amylene). Diisopropylethylamine (2.5 equiv., 57 μl) and 2-cyano-*N*,*N*-diisopropylphosphoramidochloridite (1.5 equiv., 78 mg) dissolved in dichloromethane (0.5 ml) was added to the mixture and stirred at room temperature for 1 h. The reaction was monitored by TLC (ethyl acetate/hexane/triethylamine, 45/45/1, v/v/v). The crude material was poured onto ethyl acetate and the organic phase was washed

twice with $NaHCO_3$ solution and water. Pure phosphoramidite (96 mg, yield=50%) was obtained after purification by flash chromatography (ethyl acetate/hexane/triethylamine, 45/45/1, v/v/v).

^{1}H NMR (200 MHz, $CDCl_3$) δ (ppm): 1.0 (m, 12H, CH_3^iProp), 2.44 (m, 2H, CH_2CN), 3.56 (m, 8H, CH^iProp, $CH_2\beta CN$, $2CH_2O$), 3.8 (s, 6H, CH_3O DMT), 3.8 (m, 1H, CH), 4.6 (s, 2H, CH_2CO), 6.7–7.2 (m, 13H, Har DMT), 87.2 (m, 9H, Har NDI); ^{13}C NMR (50.32 MHz, $CDCl_3$) δ (ppm): 19.8–19.9 (CH_2CN), 24.2 (CH_3^iProp), 42.0 (CH_2CO), 42.6–42.8 (CH^iProp), 49.7 (*CH*CH_2O), 54.9 (OCH_3), 57.7–58.1 (O*CH*$_2$CH$_2$), 60.8, 61.0, 61.4, 61.7 (CH*CH*$_2$O), 85.5 (Cquat DMT), 117.5 (CN), 122.8, 124.9, 125.3, 126.1, 127.3, 127.5 (CHar pyrene), 112.7, 126.4, 127.4, 128.2, 129.6 (CHar DMT), 124.4, 124.9, 129.3, 130.6, 130.7, 131.1 (Cquat ar pyrene), 135.4, 144.5, 158.1 (Cquat ar DMT), 170.3 (CO). ^{31}P NMR (200 MHz, $CDCl_3$) δ (ppm): 146.0–146.2. MS (FAB) *m/z* 858.37 ($M+Na^+$); HRMS (FAB) calcd for $C_{51}H_{54}N_3NaO_6P$ ($M+Na^+$) 858.3644, found 858.3647.

8.2.4. *N*-Methyl-*N′*-carboxymethyl-1,4,5,8-naphtalenetetracarboxylic diimide (1). Naphtalenedianhydride (3 g) was dissolved in dimethylformamide (120 ml) and glycine (1 equiv., 838 mg) and diisopropylethylamine (0.5 equiv., 1.92 ml) were then added. The reaction was stirred overnight at 90°C. The mixture was cooled and methylamine in ethanol (1.5 equiv., 2.04 ml) was added and stirred at room temperature for 3 h. The crude material was concentrated and then dissolved in water/methanol (2/1). The pH was adjusted to 3 with concentrated HCl. The residue was concentrated and then washed with methanol. The pure acid **1** was obtained by filtration (3.2 g, yield=83%). UV (MeOH) λ_{max} (nm) (ε) 373 (19,300), 353 (16,900), 232 (19,600), 205 (19,800); IR (KBr) 1704, 1668 cm^{-1}; ^{1}H NMR (200 MHz, $DMSOd_6$) δ (ppm): 3.39 (s, 3H, CH_3N), 4.7 (s, 2H, CH_2), 8.6 (dd, 4H, Har); ^{13}C NMR (50.32 MHz, DMSO-d_6) δ (ppm): 26.9 (CH_3N), 41.6 (CH_2), 125.2–126.5 (Cquat ar), 130.2–130.8 (CHar), 162.0–162.5 (CO). MS (FAB) *m/z* 339.22 (MH^+); HRMS (FAB) calcd for $C_{17}H_{11}N_2O_6$ (MH^+) 339.0617, found 339.0620.

8.2.5. *N*-Methyl-*N′*-(*N*-(2-hydroxy-1-hydroxymethyl-ethyl)-acetamide)-1,4,5,8-naphtalenetetracarboxylic diimide (N). 1 (1 g) was dissolved in dimethylformamide (200 ml), PyBOP (3 equiv., 3.8 g) and then hydroxybenzotriazole (HOBt) (2 equiv., 0.665 g), triethylamine (2 equiv., 0.684 ml) and serinol (2.5 equiv., 0.560 g) were added. The mixture was stirred at 40°C for 3 h. The reaction was monitored by TLC (methanol/CH_2Cl_2; 2/80 v/v). The crude material was concentrated. The product was purified by flash chromatography with a 10–50% gradient of methanol in dichloromethane. To eliminate the residual HOBt, the product was dispersed in acetone (30 ml) and poured onto water (150 ml). After a few hours, the diol precipitated. **N** was then filtered off (0.385 mg, yield=42%).

UV (MeOH) λ_{max} (nm) (ε) 374 (14,900), 355 (11,900), 231 (21,100); IR (KBr) 1676, 1664 cm^{-1}; ^{1}H NMR (200 MHz, DMSO-d_6) δ (ppm): 3.35 (s, 3H, CH_3N), 3.4–3.42 (d, J^3=5.54 Hz, *CH*$_2$OH), 3.7 (m, 1H, CH), 4.6 (s, 2H, *CH*$_2$CONH), 4.64 (t, J^3=5.4 Hz, 2H, OH), 8.0 (d, J^3=7.9 Hz, 1H, NH), 8.52 (s, 4H, Har); ^{13}C NMR (50.32 Hz, DMSO-d_6) δ (ppm):26.9 (CH_3N), 42.6 (*CH*$_2$-CONH), 53.2 (CH), 60.4 (CH_2OH), 125.7–126.5 (Cquat ar), 130.2–130.6 (CHar), 162.3–162.7 (*CO*N), 166.0 (*CO*NH). MS (FAB) *m/z* 412.14 (MH^+); HRMS (FAB) calcd for $C_{20}H_{17}N_3O_7$ (MH^+) 412.1144, found 412.1146.

8.2.6. *N*-Methyl-*N′*-(*N*-(2-hydroxy-1-(-*O*-4,4′-dimethoxytritylmethyl-ethyl)-acetamide))-1,4,5,8-naphtalenetetracarboxylic diimide (2b). N (250 mg) was carefully dried by three co-evaporations with pyridine and then dissolved in anhydrous pyridine (30 ml). Dimethoxytrityl chloride (0.8 equiv., 163 mg) was added under argon atmosphere and mixed at room temperature for 2 h. The reaction was monitored by TLC (ethyl acetate/hexane, 70/30, v/v). The mixture was poured onto water (30 ml), and the organic phase was extracted twice by MeOH/CH_2Cl_2 (1/2, v/v) and was then washed, dried and concentrated. Pure **2b** was obtained after purification by flash chromatography with a gradient of ethyl acetate in hexane (70–100%) in the presence of 1% triethylamine (200 mg, yield=46%).

^{1}H NMR (200 MHz, $CDCl_3$) δ (ppm): 3.2 (d, 2H, C*H*$_2$OH), 3.4 (s, 2H, C*H*$_2$O), 3.54 (s, 3H, C*H*$_3$N), 3.76 (s, 6H, C*H*$_3$O DMT), 4.0 (m, 1H, C*H*), 4.8 (s, 2H, C*H*$_2$CO), 6.67–7.25 (m, 13H, C*H*ar DMT), 8.6 (s, 4H, C*H*ar NDI); ^{13}C NMR (50.32 MHz, $CHCl_3$) δ (ppm): 27.3 (CH_3N), 43.0 (*C*H$_2$CO), 51.4 (CH), 55.1 (CH_3O DMT), 62.8–63.2 ($2CH_2O$), 86.2 (Cquat DMT), 113.1, 126.6, 127.9, 129.8 (CHar DMT), 130.7–131.1 (CHar NDI), 126.0–126.8 (Cquat ar NDI), 135.5, 144.3, 158.4 (Cquat ar DMT), 162.4–162.8 (*CO*N), 166.5 (*CO*NH). MS (FAB) *m/z* 726.23 ($M+Na^+$); HRMS (FAB) calcd for $C_{41}H_{35}N_3NaO_9$ ($M+Na^+$) 736.2270, found 736.2263.

8.2.7. *N*-Methyl-*N′*-(*N*-(2-(2-cyanoethoxy(diisopropylamino))-1-(-*O*-4,4′-dimethoxytritylmethyl-ethyl)-acetamide))-1,4,5,8-naphtalenetetracarboxylic diimide (3b). 2b (260 mg) was carefully dried by three co-evaporations with pyridine and then was diluted in anhydrous dichloromethane (3 ml, stabilized with amylene). Diisopropylethylamine (2.5 equiv., 140 ml) and 2-cyano-*N*,*N*-diisopropylphosphoramidochloridite (1.5 equiv., 115 mg) dissolved in dichloromethane (0.5 ml) was added to the mixture and stirred at room temperature for 1 h. The reaction was monitored by TLC (ethyl acetate/hexane/triethylamine, 45/45/1, v/v/v). The crude extract was poured onto ethyl acetate and the organic phase was washed twice with $NaHCO_3$ solution and water. Pure phosphoramidite (190 mg, yield=50%, R_f=0.66) was obtained after purification by flash chromatography (ethyl acetate/hexane/triethylamine, 45/45/10, v/v/v).

^{1}H NMR (200 MHz, $CDCl_3$) δ (ppm): 1.12 (m, 12H, CH_3iPr), 2.52 (m, 2H, CH_2CN), 3.52 (m, 11H, CH_2O DMT, CH_2OP, $CH_2\beta CN$, 2CH*iPr*, CH_3N), 3.75 (s, 6H, CH_3O DMT), 4.29 (m, 1H, CH), 4.8 (s, 2H, CH_2CONH), 6.7–7.2 (m, 13H, Har DMT), 8.7 (s, 4H, Har NDI); ^{13}C NMR (50.32 MHz, $CDCl_3$) δ (ppm):20.3 (CH_2CN), 24.5–24.6 (CH_3^iProp), 27.3 (CH_3N), 42.9 (CH_2CONH), 49.9 (CH), 55.1 (CH_3O), 58.6 ($CH_2\beta CN$), 61.4–62.0 (CH_2O), 86.0 (Cquat DMT), 113.0, 126.7, 127.8, 128.1, 129.9 (CHar

DMT), 126.2–126.7 (Cquat ar NDI), 130.8–131.1 (CHar NDI), 135.7, 144.5, 158.4 (C quat ar DMT), 162.5–163.0 (*CO*N), 165.7 (*CO*NH). ^{31}P NMR ($CDCl_3$) δ (ppm): 146.4–146.6. MS (FAB) *m/z* 936.33 ($M+Na^+$); HRMS (FAB) calcd for $C_{50}H_{52}N_5NaO_{10}P$ ($M+Na^+$) 936.3349, found.936.3377.

8.3. Synthesis and purification of modified oligonucleotides

All oligonucleotides were synthesized on a 0.2 μmol scale on an Expedite 8909 DNA synthesizer using conventional β-cyanoethyl phosphoramidite chemistry. The **P** and **N** modified phosphoramidites were dissolved in anhydrous acetonitrile (0.1 M final concentration), and were used with a coupling time of 15 min. The coupling efficiency was the same as that of unmodified amidite (>98). The **P**-containing oligonucleotides were deprotected by the standard procedure: standard CPG (P in 5′) were treated for 30 min with AMA (NH_4OH/methylamine, 50:50, v/v) (1 ml) at 65°C. Universal supports (GLEN RESEARCH) (P in 3′) were treated overnight with AMA (1 ml) at 55°C. The **N**-containing oligonucleotides were deprotected using the following conditions. Standard supports were treated for 4 h at rt in NH_4OH (1 ml), and universal supports were treated for 17 h at rt with a solution 0.4 M NaOH in MeOH/water (4/1) (1 ml) and then neutralized by 2 M TEAA (1.5 ml). The crude oligonucleotides deprotected in AMA or NH_4OH were then evaporated to dryness, and those treated by NaOH were precipitated in butanol. The crude oligonucleotides were purified by electrophoresis on denaturing polyacrylamide gels. The pure samples were desalted through reverse phase maxi-clean cartridges (C18, Altech).

8.4. UV-monitored melting experiments

Thermal denaturation of modified oligonucleotides were monitored on a Cary 1 spectrophotometer interfaced with a Peltier effect device that controled the temperature to within ±0.1°C. Denaturation of the samples (1 μM final concentration) in 20 mM cacodylate buffer, pH 7.3, at 20°C containing 140 mM potassium chloride, 20 mM sodium chloride and 3 mM magnesium chloride was achieved by increasing the temperature by 0.5°C min^{-1} from 5 to 95°C and was monitored at 260 nm. The melting temperature, T_m, was taken as the peak of the first derivative of the UV melting curves. Samples at 1 μM final were boiled for 1 min, kept for 10 min at 4°C, and then for 10 min at rt. The experiment started 30 min later at this temperature of 5°C. At 260 nm a molar extinction coefficient of 2.04×10^4 mol^{-1} l cm^{-1} was used for P and 4.17×10^4 mol^{-1} l cm^{-1} for N.

8.5. Fluorescence measurements

The fluorescence of 0.1 μM oligonucleotides was recorded in the above mentioned buffer on a PTI spectrofluorimeter. Temperature was controlled and set to 23°C with a Peltier effect device. Spectral data were corrected both in excitation and emission and recorded at 50 nm min^{-1}.

8.6. Molecular modeling studies

Molecular mechanic energies were calculated using the Amber force field. The simulations were performed with a distance-dependent dielectric permittivity ($1/r$) to simulate the screening induced by solvent molecules.[10] Several initial structures were built as extended, stacked or intercalated species with the atom charge given by Amber for hairpin and with atom charges calculated by using the AM1 semi-empirical method for pyrene and naphtalene diimide residues. To compare the results, the most stable structures of each species were retained. The structures were energy-minimized using 1000 steps of the 'steepest descent' algorithm followed by steps of the Polak–Ribiëre 'conjugate gradient' until the energy gradient was smaller than 0.02 kcal mol^{-1} $Å^{-1}$.

Acknowledgments

We thank Dr Jean-Jacques Toulmé for helpful discussions.

References

1. Petersheim, M.; Turner, D. H. *Biochemistry* **1983**, *22*, 256–263.
2. Wang, A. H. J. *Nucleic Acids Mol. Biol.* **1987**, *1*, 53–69.
3. Guckian, K. M.; Schweitzer, B. A.; Ren, R. X. F.; Sheils, C. J.; Tahmassebi, D. C.; Kool, E. T. *J. Am. Chem. Soc.* **2000**, *122*, 2213–2222.
4. Nguyen, J. Q.; Iverson, B. L. *J. Am. Chem. Soc.* **1999**, *121*, 2639–2640.
5. Winnik, F. M. *Chem. Rev.* **1993**, *93*, 587–614.
6. Benhida, R.; Devys, M.; Fourrey, J. L.; Lecubin, F.; Sun, J. S. *Tetrahedron Lett.* **1998**, *39*, 6167–6170.
7. Ducongé, F.; Toulmé, J. J. *RNA* **1999**, *5*, 1605–1614.
8. Peters, A. T.; Bide, M. J. *Dyes Pigment* **1985**, *6*, 349–375.
9. Newcomb, L. F.; Gellman, S. H. *J. Am. Chem. Soc.* **1994**, *116*, 4993–4994.
10. Guenot, J.; Kollman, P. A. *Protein Sci.* **1992**, *1*, 1185–1205.